Evolution of octupole collectivity in ^{221}Th

S. K. Tandel,* M. Hemalatha, A. Y. Deo,† and S. B. Patel
UM-DAE Centre for Excellence in Basic Sciences, Mumbai 400098, India

R. Palit, T. Trivedi, J. Sethi, and S. Saha
Department of Nuclear and Atomic Physics, Tata Institute of Fundamental Research, Mumbai 400005, India

D. C. Biswas and S. Mukhopadhyay
Nuclear Physics Division, Bhabha Atomic Research Centre, Mumbai 400085, India

(Received 27 December 2012; revised manuscript received 6 February 2013; published 21 March 2013)

Reflection-asymmetric octupole structures are studied in the transitional nucleus ^{221}Th. There are several modifications at intermediate spins to the previously reported yrast structure. The level scheme is considerably extended with yrast states up to $(39/2)\hbar$ established. A nonyrast octupole structure is identified which does not constitute a parity doublet with the yrast states, unlike those observed in some of the heavier odd-A Th isotopes. This is attributed to the low K value of the ground-state configuration. The strength of octupole correlations and quadrupole collectivity is found to vary with spin. The role of nucleon alignments in influencing collective properties is explored through cranking calculations incorporating octupole deformation.

DOI: 10.1103/PhysRevC.87.034319 PACS number(s): 21.10.Re, 23.20.Lv, 25.70.Gh, 27.90.+b

I. INTRODUCTION

The Ra-Th region around $A \approx 220$ provides some of the best examples of well-developed octupole shapes in nuclei. Experimental signatures of octupole correlations are low-lying negative-parity levels and enhanced strengths for $E1$ transitions between positive- and negative-parity states. The strong octupole collectivity in this region is due to the presence of orbitals, which differ by Δj, $l = 3$, near the Fermi surface for both protons and neutrons. In the case of neutrons, the $j_{15/2}$ and $g_{9/2}$ orbitals beyond the $N = 126$ shell closure contribute, whereas, in the case of protons, the $i_{13/2}$ and $f_{7/2}$ orbitals beyond the $Z = 82$ shell gap are involved. The excited-level structure near the center of this region of enhanced octupole collectivity constitutes an excellent illustration of reflection-asymmetric shapes in nuclei. In odd-A nuclei with $K \neq 0$, this phenomenon is manifested in terms of so-called parity-doublet structures [1,2]. These are near-degenerate states with identical spins and opposite parities, and a large connecting $E3$ matrix element. For such structures, the intrinsic Hamiltonian does not commute with the parity operator due to the presence of odd-multipole components in the nuclear deformation, but it is, however, invariant under the combined operations of parity and rotation.

Initial evidence of octupole correlations in this region at low spin came from decay studies [3] up to Pa ($Z = 91$). Several high-spin investigations focused on doubly even isotopes of Rn ($Z = 86$) to Th ($Z = 90$) (e.g., Refs. [4,5]). Studies of odd-A isotopes of Rn, Ra, and Th, and odd-A and odd-odd isotopes of Fr and Ac (e.g., Refs. [6–10]), were reported. Octupole correlations varied from vibrationlike to the appearance of near-static octupole deformation in some cases. These observations were supported by a variety of theoretical approaches such as microscopic many-body calculations [1], the particle-rotor model [11], and Woods-Saxon calculations using a reflection-asymmetric mean field considering odd-multipole deformations (β_λ) with λ up to 7 [12]. Based on the location of both neutron and proton Fermi levels, the octupole strength is found to vary, with the region around $Z = 88$ and $N = 134$ exhibiting the strongest effects. The role of an odd valence nucleon on the stability of octupole deformation was also investigated [3].

With increase in neutron number beyond $N = 126$, the nuclear shape changes from spheroidal to deformed, with primarily quadrupole and octupole degrees of freedom. Mean-field calculations incorporating higher-order deformations ($\lambda \geqslant 4$) [12] indicate that there is substantial contribution from these degrees of freedom as well. Nuclei around $N = 130$ are transitional in nature, with effects of the shell gap at $N = 126$ still evident, quadrupole collectivity not fully developed, and octupole correlations being enhanced. This leads to quite uncommon shape competition effects both at low and high spins. Recently, an excitation mechanism was proposed [13,14] to explain the structure of transitional nuclei wherein the yrast states are described as quadrupole waves (also termed *tidal waves*) running over the nuclear surface, with gain in angular momentum attributed to an increase in deformation at a roughly constant angular velocity. Furthermore, it was suggested [15] that nuclei in the $A \approx 226$ region can be understood in terms of rotation-induced condensation of octupole phonons, which have their angular momentum aligned along the rotational axis leading to a heart shape rather than the more commonly invoked reflection-asymmetric pear shape.

There are several aspects to the motivation for this work. Odd-A, proton-rich isotopes, viz., ^{217,219,221}Th [7,16,17], are not as well studied in comparison with some of the doubly even or heavier odd-A isotopes. For ^{217,219}Th, a relatively small

*sujit.tandel@cbs.ac.in
†Present address: Department of Physics, Indian Institute of Technology, Roorkee 247667, India.

number of excited states up to intermediate spins have been identified thus far. In the case of ^{221}Th, states at intermediate spins had not been firmly established from the previous work [7], and only one sequence of interleaved positive- and negative-parity states had been isolated [7], in contrast to ^{223,225}Th [7,18] wherein parity doublet structures were observed to high spins. The coexistence and competition between quadrupole and octupole collectivity and their evolution with spin are of particular interest. A more recent work [19] suggests modifications at intermediate spins to the yrast structure reported previously [7], and reports the observation of a different, nonyrast, alternating-parity sequence. Furthermore, the role of nucleon alignments in influencing shape changes at high spins can be studied in a regime where octupole correlations are substantial.

II. EXPERIMENT AND DATA ANALYSIS

Excited states in ^{221}Th were populated through the ^{208}Pb(^{16}O, $3n$) reaction, at a beam energy of 86 MeV. The target was an isotopically enriched (≈99.6%) ^{208}Pb foil with 5.5 mg/cm^2 thickness. The ^{16}O beam was delivered by the 14UD BARC-TIFR Pelletron at Mumbai, India. The Indian National Gamma Array (INGA) was used to detect γ rays emitted by the reaction products. INGA consisted of 19 Compton-suppressed clover Ge detectors at the time of the experiment. Although γ rays from fragments following the fission of the ^{224}Th compound nucleus constituted the majority of the γ-γ coincidence events detected, the $3n$ channel leading to ^{221}Th was the primary evaporation residue. The choice of the beam energy was based on PACE4 calculations and results from the previous measurement [7]. The data were recorded using a triggerless digital data acquisition system based on XIA Pixie-16 modules [20] and were sorted into RADWARE-compatible [21] γ-γ matrices and γ-γ-γ cubes using the sorting routine MARCOS (Multi Parameter Coincidence Search) developed at TIFR. A total of approximately 110 million γ-γ-γ events were recorded to disk. In the absence of additional selectivity like the detection of recoiling residual nuclei, a judicious combination of double-gated γ spectra along with Th K x-ray gated spectra was crucial in building up the decay scheme. Directional correlation from oriented states (DCO) [22] information from four detectors at 90° and three detectors at 157° with respect to the beam direction was obtained by creating angle-dependent γ-γ matrices. The DCO ratio ($R_{\rm DCO}$) for this experiment was defined as

$$R_{\rm DCO} = \frac{I_{\gamma_1}\ (\text{at } 157^\circ \text{ gated by } \gamma_2 \text{ at } 90^\circ)}{I_{\gamma_1}\ (\text{at } 90^\circ \text{ gated by } \gamma_2 \text{ at } 157^\circ)}. \qquad (1)$$

With gates on stretched quadrupole transitions, the $R_{\rm DCO}$ value was found to be around 0.5 and 1.0 for stretched dipole and quadrupole transitions, respectively. The measured DCO ratios allowed for confirmation of multipolarity of several intense transitions identified from the previous work [7], and its assignment for a few newly identified γ rays.

III. RESULTS

Only one sequence each of positive- and negative-parity states was identified from the previous study of ^{221}Th [7]. Several transitions in the positive-parity sequence were tentatively assigned, and the ground-state spin was not conclusively established. The transitions established at low spins were confirmed in the present work; however, several transitions at intermediate spins were found to be incorrectly assigned. The decay scheme was extended up to spin $(39/2)\hbar$ in the yrast sequence. In addition, a nonyrast structure with interleaved positive- and negative-parity sequences was identified, with transitions up to spin $(25/2)\hbar$. Several transitions connecting the yrast and nonyrast structures were established. A total of 23 new transitions were identified in the present work.

The ground-state spin of ^{221}Th was assigned to be $(7/2)^+$. Though there are several strong arguments in support of this scenario, experimental considerations alone are not sufficient for an unambiguous assignment. A detailed discussion about this aspect is presented in the next section. The subsequent description is based on a $(7/2)^+$ ground-state spin assignment.

Figure 1 illustrates the transitions in the yrast (top panel) and nonyrast (bottom panel) structures. The partial decay scheme established for ^{221}Th based on observed coincidences and intensity considerations is presented in Fig. 2. Both $E1$ and $E2$ transitions reported to deexcite the $(31/2)^+$ and $(33/2)^-$ states [7] were modified. The yrast positive-parity structure now consists of the 433-, 474-, and 513-keV $E2$ transitions (in that order) feeding the $(27/2)^+$ state. In the negative-parity structure, the 485-keV transition deexciting the $(33/2)^-$ state is replaced by the 509-keV γ ray. The 485-keV transition is placed elsewhere in the decay scheme. Furthermore, the 274-, 235-, and 239-keV $E1$ γ rays are newly identified interband transitions in the yrast structure. Coincidence spectra supporting the revision and extension of

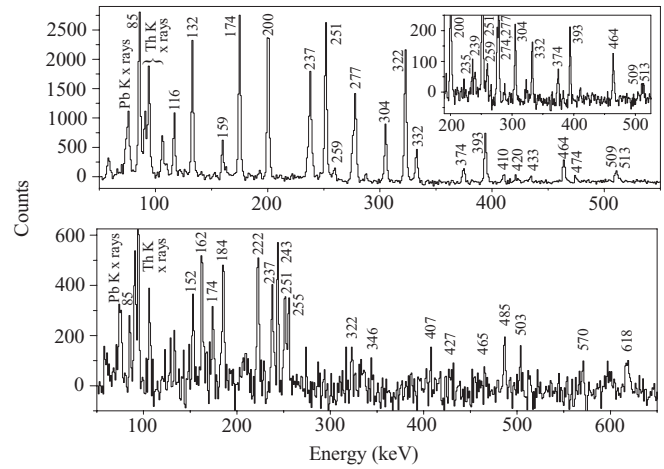

FIG. 1. Summed double-gated spectra illustrating transitions in the yrast and nonyrast structures (top and bottom, respectively). Most of the low-energy γ rays have $E1$ character, whereas the higher-energy transitions have $E2$ nature. The inset in the top panel shows transitions in coincidence with the 322-keV γ ray in the yrast structure and highlights the closely spaced transitions at 235 and 239 keV, 274 and 277 keV, and 509 and 513 keV. Four of the highest-energy transitions in the bottom panel deexcite the nonyrast to yrast states. Some coincident γ rays from the yrast structure are also seen in the bottom panel. Both Th and Pb (target) K x rays are visible.

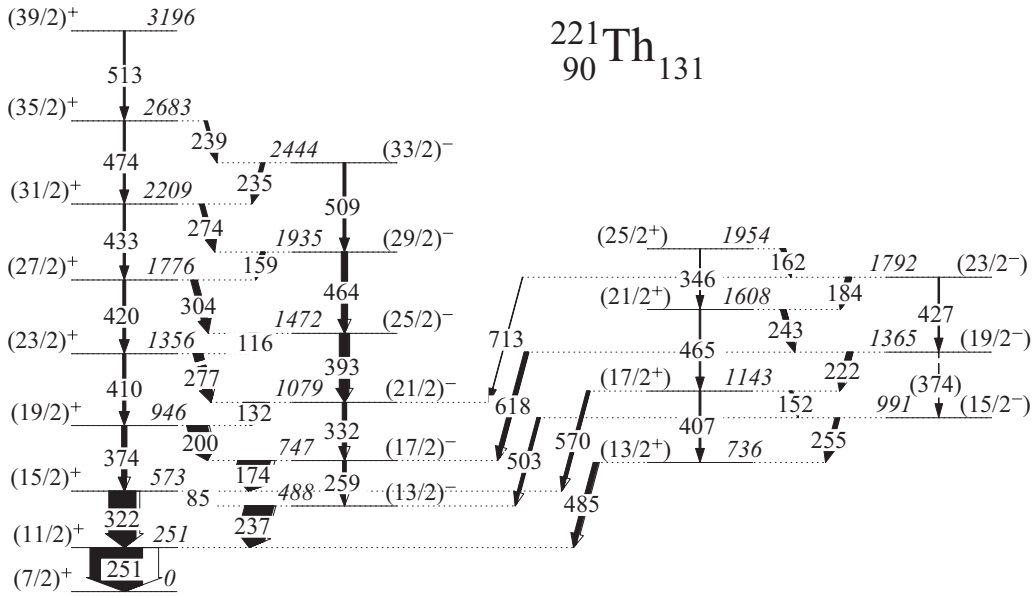

FIG. 2. Partial decay scheme for ^{221}Th. Transition energies are in keV, and rounded off to the nearest integer. The widths of solid and open regions of the arrows are proportional to the γ and internal conversion intensities, respectively, of the transitions. Spin-parity assignments are tentative (indicated by parentheses), though there is strong evidence for the chosen $(7/2)^+$ ground-state assignment. The yrast structure on the left was significantly modified at intermediate spins and extended up to the $(39/2)^+$ state. The nonyrast structure on the right is newly established from this work.

the previously reported yrast structure are shown in Fig. 3. No evidence for the 170-, 316-, and 485-keV transitions reported earlier [7] is visible in coincidence spectra gated on the 304- and 464-keV transitions [Figs. 3(a) and 3(b), respectively]. The newly assigned $E1$ and $E2$ transitions listed above are, however, clearly seen in Fig. 3.

A new nonyrast structure is identified, and linking transitions (485, 503, 570, 618, and 713 keV) to the yrast states are also established. The extent of population of the nonyrast states is about 20–25% that of the yrast structure and the ratios of the intensities of $E1$ and corresponding $E2$ transitions in the two structures is quite similar (Fig. 1). All the transitions in the nonyrast structure are newly identified, viz., the 152-, 162-, 184-, 222-, 243-, and 255-keV $E1$ γ rays and the 346-, 407-, 427-, and 465-keV $E2$ transitions. The 374-keV γ ray is tentatively placed in the decay scheme. The transitions linking some of the nonyrast states to the yrast structure are illustrated in Fig. 4. The 485-, 503-, and 618-keV transitions deexciting the $(13/2^+)$, $(15/2^-)$, and $(19/2^-)$ states in the nonyrast structure are quite prominent.

The spin and parity of the newly identified nonyrast states are tentative since experimental considerations alone do not lead to conclusive assignments. These assignments are also based on the similarity of the nature of the observed band structures to each other and those identified in the $N = 131$ isotone ^{219}Ra [23], and in addition, the decay pattern to the yrast states. The data suggest dipole character for the 485-keV transition linking the lowest observed nonyrast state to the yrast structure. The DCO ratio for this γ ray, with a gate on the 251-keV $E2$ transition, was determined to be 0.60(7). Similar values have been determined for the 174- and 200-keV $E1$ transitions in the yrast structure, i.e., 0.56(2) and 0.53(3),

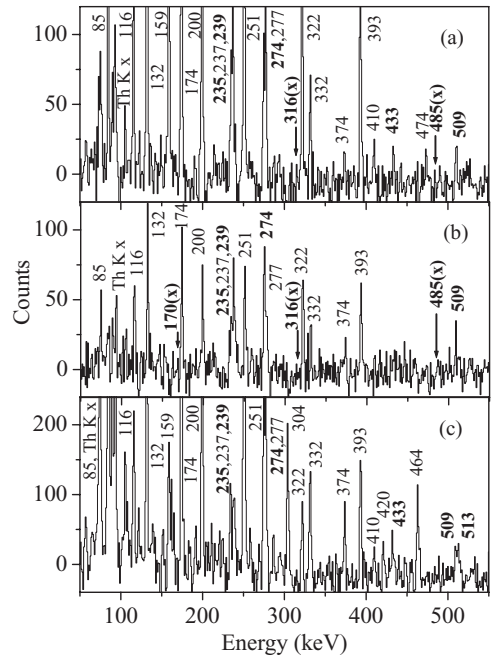

FIG. 3. Spectra illustrating transitions at high spins in the yrast structure, including revisions to the previously reported level scheme [7]. Transitions incorrectly placed in the previous work and ones identified from the present experiment are indicated in bold. The cross (**x**) sign in parentheses indicates an absence of evidence of a previously reported transition. Summed coincidences of the following γ rays with several low-lying, intense transitions in the yrast structure are displayed: (a) $(27/2)^+ \rightarrow (25/2)^-$, 304-keV transition; (b) $(29/2)^- \rightarrow (25/2)^-$, 464-keV transition; (c) $(33/2)^- \rightarrow (31/2)^+$, 235-keV transition, and $(35/2)^+ \rightarrow (33/2)^-$, 239-keV transition. More details are in the text.

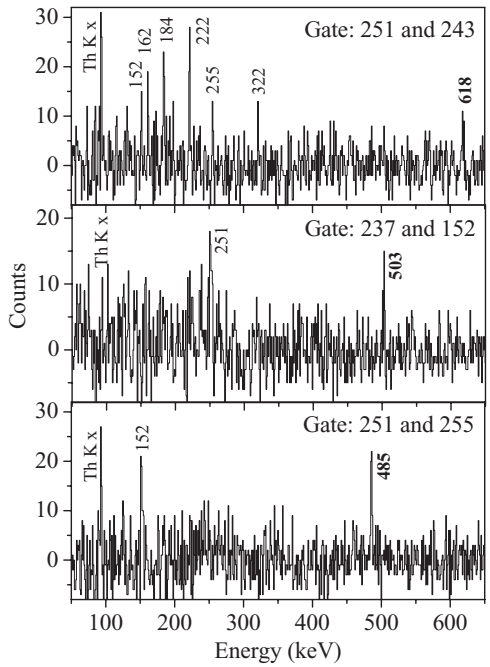

FIG. 4. Double-gated spectra illustrating some of the linking transitions (labeled in bold) from the nonyrast to the yrast states.

respectively. This implies a probable (13/2) assignment for the 736-keV state deexcited by the 485-keV transition. Hints of the parity assignment for the nonyrast states may be obtained by comparing the Th K x-ray intensity in spectra gated on the transitions in the nonyrast structure and those linking it to the yrast states. The linking transitions may have either $M1/E2$ or $E1$ multipolarity. For predominantly $M1$ multipolarity, the conversion coefficient would be quite considerable ($\approx$0.2), as opposed to the small value ($\approx$0.01) expected for $E1$ transitions of the same energy. The intensity of K x rays in spectra gated on transitions within the nonyrast structure (particularly the lower-energy, $E1$ transitions) is expected to be considerably more, with $M1$ as compared to $E1$ multipolarity for the linking transitions. A comparison of this K x-ray intensity with that observed in spectra gated on the linking transitions, where coincidences with only the γ branch of these transitions are necessarily considered, was carried out. This comparison reveals that the K x-ray intensity in the former case is consistently seen to be significantly higher, supporting $M1/E2$ rather than $E1$ multipolarity for the linking transitions. The above arguments are clearly qualitative and do not lead to an unambiguous assignment of parity for the nonyrast states. Higher statistics data would be required for the measurement of linear polarization of the linking transitions and a conclusive determination of parity.

IV. DISCUSSION

A. Ground-state spin assignment

The assignment of ground-state spin for several nuclei in the transitional region around $N = 130$ is a topic that has been extensively discussed [7,8,11,12,23]. Theoretical considerations or systematics alone do not lead to an unambiguous assignment because it has been debated whether the weak-, intermediate-, or strong-coupling scenarios are applicable for the $N = 131$ isotones, ^{219}Ra and ^{221}Th. Reflection-asymmetric particle-rotor model calculations [11] indicate that the $\Omega = 1/2$, $i_{11/2}$ neutron orbital has the dominant contribution to the ground state. There is strong Coriolis coupling between the $K = 1/2$ and $K = 3/2, 5/2$ components, which when combined with the large decoupling expected for the $K = 1/2$ orbital leads to an $I^\pi, K^\pi = 7/2^+, 1/2^+$ ground state. Mean-field calculations using a Woods-Saxon potential [12] predict a strong $K = 1/2$ component in the ground state, with the $K = 3/2$ and 5/2 states about 200 keV above the ground state. Studies of α decay, leading to the $N = 131$ isotone ^{219}Ra [24,25], constrain the ground-state spin for this nucleus to either $7/2^+$ or $11/2^+$. As mentioned in the more recent study of ^{219}Ra and elsewhere [23,26], a $11/2^+$ spin assignment for the ground state in the reflection-asymmetric strong-coupling scenario is excluded by the fact that the decoupling parameter would then be unphysically large. The α decay of both ^{225}U and ^{221}Th [16] were observed; however, the data do not aid determination of spins of the states involved. Considerations similar to those for ^{219}Ra, mentioned above, are expected to hold for ^{221}Th, leading to a very likely assignment of $7/2^+$ for the ground state, with the intermediate-coupling scheme being valid. Because the ground-state spin assignment is not completely unambiguous, spins for all the states shown in the decay scheme (Fig. 2) are in parentheses.

B. Octupole and quadrupole collectivity

For rotating nuclei with reflection-asymmetric shapes, because parity is not a good quantum number, the quantum number associated with the combined operations of parity and rotation referred to as simplex (s) is commonly employed [27]. In odd-A nuclei, two sequences each of interleaved positive- and negative-parity states with $s = -i$ and $s = +i$, referred to as parity doublet structures, are expected. A notable feature of the ^{221}Th decay scheme is the absence of parity doublet structures similar to those observed in heavier odd-A isotopes, ^{223,225}Th [7,18]. Parity doublets are also absent in the $N = 131$ isotone ^{219}Ra [23], which, for both nuclei, is consistent with the strong decoupling resulting from a dominant $K = 1/2$ contribution to the structure built on the ground state, as mentioned earlier. A similar situation is realized in ^{227}Th [28,29], where parity doublets are absent as a result of a $K = 1/2$ ground-state configuration. The nonyrast structure observed in ^{221}Th also quite likely has $K = 1/2$ and is elevated in energy because of the large decoupling characteristic of a $K = 1/2$ configuration. However, a different value of K for the nonyrast states cannot be definitely ruled out.

A common feature that emerges from the moments of inertia (MOI) for the observed band structures in the $N = 131$ isotones ^{219}Ra and ^{221}Th is that the MOI of the negative-parity states is consistently higher than that of positive-parity states with the same simplex (Fig. 5) at low spins. An explanation of this phenomenon arises from self-consistent Hartree-Fock calculations [30], wherein the negative-parity structures are predicted to have larger quadrupole deformation than the corresponding positive-parity ones, leading to increased MOI.

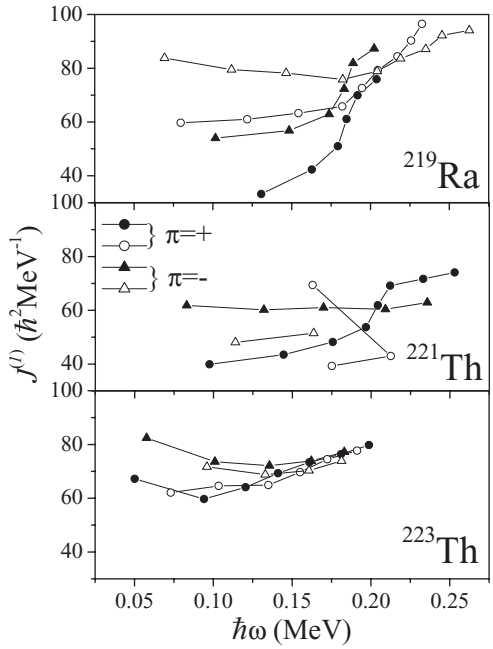

FIG. 5. Kinematic moment of inertia (MOI) for both positive- and negative-parity structures in the $N = 131$ isotone ^{219}Ra, and ^{221,223}Th. A pronounced increase in MOI is evident for both ^{219}Ra and ^{221}Th around a rotational frequency of $\hbar\omega \approx 0.2$ MeV, particularly for the positive-parity structures.

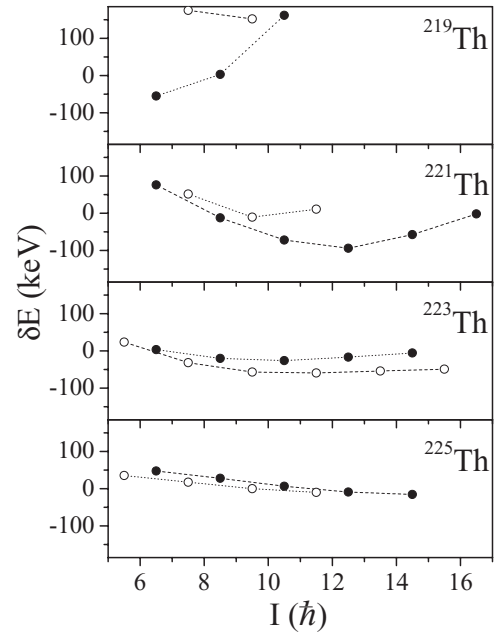

FIG. 6. The energy splitting between positive- and negative-parity states for octupole structures in Th isotopes. The solid circles correspond to simplex $s = -i$, while the open circles denote $s = +i$. A value of $\delta E = 0$ signifies static octupole deformation. For ^{221}Th, there is a large separation in energy between the yrast and nonyrast structures with similar spins (Fig. 2); therefore, the simplex quantum number cannot be unambiguously assigned, unlike for example, in ^{223,225}Th.

At higher spins, the experimental values approach each other, indicating increase in quadrupole collectivity for the positive-parity states. For ^{221}Th and to some extent in ^{219}Ra, the MOI of the yrast positive-parity states exceeds that of the negative-parity states at high spins (Fig. 5). This is accompanied by loss of intensity in the negative-parity structure, probably because of a decrease in octupole collectivity.

For nuclei with $N < 130$, the shape is spheroidal (smaller β_2), whereas for $N > 132$, the magnitude of the quadrupole deformation is significantly higher than the octupole deformation. For nuclei in the transitional region like ^{221}Th ($N = 131$), the magnitude of the quadrupole and octupole deformations is predicted to be quite similar ($\beta_2 \approx 0.1$, $\beta_3 \approx 0.1$) [12]. For odd-A nuclei with static octupole deformation, it is expected that the displacement in energy (δE) between interleaved positive- and negative-parity states will be close to zero [27], where δE is given by

$$\delta E = E(I^-) - \tfrac{1}{2}\{E[(I+1)^+] + E[(I-1)^+]\}. \qquad (2)$$

The systematic variation of this quantity for several odd-A Th isotopes is shown in Fig. 6. It is evident that the energy difference is closest to zero around neutron number $N = 134$, for which octupole correlations are expected to be most pronounced. For ^{221}Th, δE varies with spin, being close to zero at low and high spins, and deviating from zero at intermediate spins for the yrast states, indicative of vibrationlike octupole character. Furthermore, there is a pronounced decrease in intensity in the negative-parity sequence at high spin: no transitions could be identified beyond the $(33/2)^-$ state. In contrast, a more regular decrease in intensity is observed in the positive-parity sequence up to the highest observed $(39/2)^+$ state. The above features are associated with a pronounced increase in MOI for the positive-parity structure at a rotational frequency $\hbar\omega \approx 0.2$ MeV (Fig. 5), as a result of which the difference in energy between the positive- and negative-parity states gradually approaches zero. The higher MOI can be correlated with either increasing quadrupole deformation or rotation alignment of nucleons.

The intrinsic electric dipole moment (D_0) values deduced for the yrast structure are illustrated in Fig. 7. The dipole

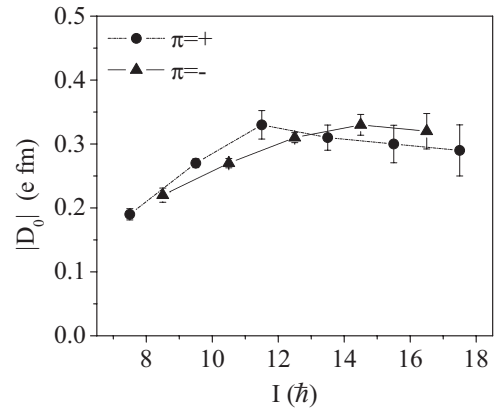

FIG. 7. Intrinsic electric dipole moments as a function of spin deduced from measured intensities of $E1$ and $E2$ transitions in the yrast structure of ^{221}Th (details about the calculation are in the text).

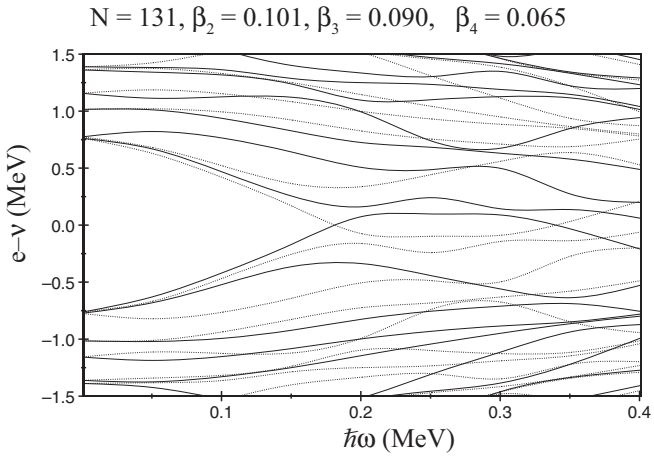

FIG. 8. Neutron quasiparticle levels from Woods-Saxon cranking calculations for ^{221}Th. Solid lines denote simplex $s = +i$, while dotted lines correspond to $s = -i$. The values of ground-state deformation parameters are taken from Ref. [12].

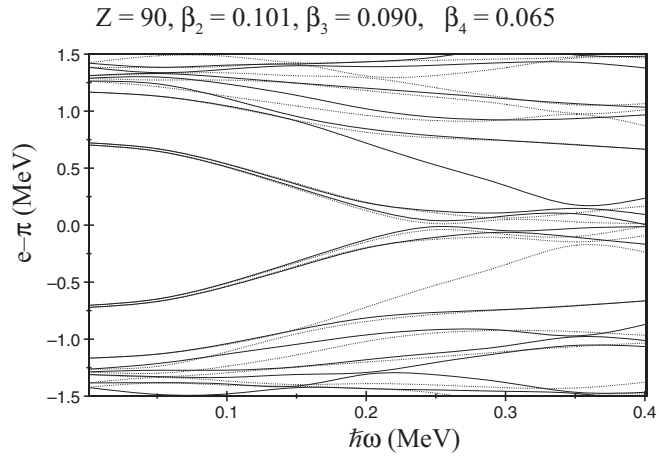

FIG. 9. Similar to Fig. 8, but for protons.

moments D_0 can be obtained from the measured $B(E1)/B(E2)$ ratio for transitions from a given state through the relation

$$\left(\frac{D_0}{Q_0}\right)^2 = \frac{5}{8}\frac{B(E1)}{B(E2)}\frac{(I+K-1)(I-K-1)}{(2I-1)(I-1)}, \qquad (3)$$

where the experimental or semiempirical Grodzins value [31] may be adopted for the quadrupole moment Q_0. For ^{221}Th, a value of $Q_0 = 415e$ fm^2 as adopted in Ref. [7] was used. For the positive-parity states, a small decrease in D_0 beyond $\hbar\omega = 0.2$ MeV from a maximum of $0.33e$ fm (Fig. 7) is evident, while for the negative-parity states D_0 is almost constant at the highest spins. If the increase in MOI for the positive-parity states is correlated with a larger value of quadrupole deformation, then the assumption of fixed Q_0 in Eq. (2) may not be valid for the entire band.

It should be noted that although the highest spins reached in odd-A isotopes ^{221}Th and beyond are quite similar, somewhat higher rotational frequencies are achieved in ^{221}Th (up to 0.25 MeV). This is particularly relevant because nucleon alignments in these nuclei occur beyond 0.20 MeV. This aspect is illustrated in our calculations of the neutron and proton quasiparticle levels as a function of rotational frequency for ^{221}Th (Figs. 8 and 9). The cranking calculations were performed using the universal parametrization of the Woods-Saxon potential, including deformations (β_λ) up to $\lambda = 4$. These indicate nucleon alignments beyond 0.20–0.25 MeV. It has been observed in several instances that strong octupole collectivity is correlated with delay or absence of nucleon alignments [32]. In ^{221}Th, the odd valence neutron occupies the $i_{11/2}$ orbital; therefore, rotation alignment of nucleons in this orbital is blocked. When octupole deformation is considerable, the $j_{15/2}$ neutron orbital approaches the Fermi surface only for higher neutron numbers [11], or at higher rotational frequencies. The $i_{13/2}$ proton alignment is expected at $\hbar\omega \approx 0.25$ MeV (Fig. 9). It is therefore necessary to establish the decay scheme to even higher rotational frequencies for a conclusive understanding of changing quadrupole deformation and the role of nucleon alignments.

V. SUMMARY

The high-spin structure of the reflection-asymmetric, odd-A nucleus ^{221}Th was investigated and a nonyrast octupole structure was identified. Several changes were made to the previously reported yrast states at intermediate spins, with levels up to $(39/2)\hbar$ being established. Near-degenerate parity doublet structures similar to those observed in the heavier odd-A Th isotopes ^{223,225}Th are not evident in ^{221}Th. The observed structures are similar to those in the $N = 131$ isotone ^{219}Ra, and the ones in ^{227}Th with a $K = 1/2$ ground state. Several arguments support a $7/2^+$ assignment for the ground state in ^{221}Th, with a dominant contribution from a $K = 1/2$ configuration. The nonyrast states exhibit a vibrationlike pattern indicative of the small underlying quadrupole deformation. The moment of inertia of the negative-parity sequence is found to be higher than the corresponding positive-parity one, a feature consistently observed across many nuclei in this region. This is attributed to a larger underlying quadrupole deformation for the negative-parity states. The moment of inertia of the positive-parity states shows a pronounced increase at higher spins, while the intensity in the negative-parity sequence decreases rapidly, features that can be interpreted as an increase in quadrupole as compared to octupole collectivity. Cranking calculations indicate nucleon alignments beyond 0.20–0.25 MeV. It will be instructive to explore the structure of nuclei well beyond 0.25 MeV in this region in order to delineate and understand the effects of predicted $i_{13/2}$ proton and $j_{15/2}$ neutron alignments.

ACKNOWLEDGMENTS

The authors would like to thank the crew at the BARC-TIFR Pelletron, INGA support staff at TIFR, and all others who have contributed to the INGA collaboration. This work was partially supported by the Department of Science and Technology, Government of India (Grant No. IR/S2/PF-03/2003-III).

[1] R. R. Chasman, Phys. Rev. Lett. **42**, 630 (1979).

[2] S. Cwiok and W. Nazarewicz, Phys. Lett. B **224**, 5 (1989).

[3] I. Ahmad and P. A. Butler, Annu. Rev. Nucl. Part. Sci. **43**, 71 (1993); P. A. Butler and W. Nazarewicz, Rev. Mod. Phys. **68**, 349 (1996), and references therein.

[4] J. F. C. Cocks, D. Hawcroft, N. Amzal, P. A. Butler, K. J. Cann, P. T. Greenlees, G. D. Jones, S. Asztalos, R. M. Clark, M. A. Deleplanque, R. M. Diamond, P. Fallon, I. Y. Lee, A. O. Machiavelli, R. W. Macleod, F. S. Stephens, P. Jones, R. Julin, R. Broda, B. Fornal, J. F. Smith, T. Lauritsen, P. Bhattacharya, and C. T. Zhang, Nucl. Phys. A **645**, 61 (1999).

[5] J. F. Shriner, Jr., P. D. Cottle, J. F. Ennis, M. Gai, D. A. Bromley, J. W. Olness, E. K. Warburton, L. Hildingsson, M. A. Quader, and D. B. Fossan, Phys. Rev. C **32**, 1888 (1985).

[6] N. Roy, D. J. Decman, H. Kluge, K. H. Maier, A. Maj, C. Mittag, J. Fernandez-Niello, H. Puchta, and F. Riess, Nucl. Phys. A **426**, 379 (1984).

[7] M. Dahlinger, E. Kankeleit, D. Habs, D. Schwalm, B. Schwartz, R. S. Simon, J. D. Burrows, and P. A. Butler, Nucl. Phys. A **484**, 337 (1988).

[8] P. D. Cottle, M. Gai, J. F. Ennis, J. F. Shriner, Jr., D. A. Bromley, C. W. Beausang, L. Hildingsson, W. F. Piel, Jr., D. B. Fossan, J. W. Olness, and E. K. Warburton, Phys. Rev. C **36**, 2286 (1987).

[9] F. Cristancho, J. X. Saladin, M. P. Metlay, W. Nazarewicz, C. Baktash, M. Halbert, I-Y. Lee, D. F. Winchell, S. M. Fischer, and M. K. Kabadiyski, Phys. Rev. C **49**, 663 (1994).

[10] M. E. Debray, M. A. Cardona, D. Hojman, A. J. Kreiner, M. Davidson, J. Davidson, H. Somacal, G. Levinton, D. R. Napoli, S. Lenzi, G. de Angelis, M. De Poli, A. Gadea, D. Bazzacco, C. Rossi-Alvarez, and N. Medina, Phys. Rev. C **62**, 024304 (2000).

[11] G. A. Leander and Y. S. Chen, Phys. Rev. C **37**, 2744 (1988).

[12] S. Cwiok and W. Nazarewicz, Nucl. Phys. A **529**, 95 (1991).

[13] S. Frauendorf, Y. Gu, and J. Sun, Int. J. Mod. Phys. E **20**, 465 (2011)..

[14] W. Reviol, C. J. Chiara, M. Montero, D. G. Sarantites, O. L. Pechenaya, M. P. Carpenter, R. V. F. Janssens, T. L. Khoo, T. Lauritsen, C. J. Lister, D. Seweryniak, S. Zhu, and S. G. Frauendorf, Phys. Rev. C **74**, 044305 (2006).

[15] S. Frauendorf, Phys. Rev. C **77**, 021304(R) (2008); X. Wang, R. V. F. Janssens, M. P. Carpenter, S. Zhu, I. Wiedenhöver, U. Garg, S. Frauendorf, T. Nakatsukasa, I. Ahmad, A. Bernstein, E. Diffenderfer, S. J. Freeman, J. P. Greene, T. L. Khoo, F. G. Kondev, A. Larabee, T. Lauritsen, C. J. Lister, B. Meredith, D. Seweryniak, C. Teal, and P. Wilson, Phys. Rev. Lett. **102**, 122501 (2009).

[16] P. Kuusiniemi, F. P. Hessberger, D. Ackerman, S. Hofmann, B. Sulignano, I. Kojouharov, and R. Mann, Eur. Phys. J. A **25**, 397 (2005).

[17] W. Reviol, D. G. Sarantites, C. J. Chiara, M. Montero, R. V. F. Janssens, M. P. Carpenter, T. L. Khoo, T. Lauritsen, C. J. Lister, D. Seweryniak, S. Zhu, O. L. Pechenaya, and S. G. Frauendorf, Phys. Rev. C **80**, 011304(R) (2009).

[18] J. R. Hughes, R. Tolle, J. De Boer, P. A. Butler, C. Gunther, V. Grafen, N. Gollwitzer, V. E. Holliday, G. D. Jones, C. Lauterbach, M. Marten-Tolle, S. M. Mullins, R. J. Poynter, R. S. Simon, N. Singh, R. J. Tanner, R. Wadsworth, D. L. Watson, and C. A. White, Nucl. Phys. A **512**, 275 (1990).

[19] W. Reviol, D. G. Sarantites, X. Chen, M. Montero, O. L. Pechenaya, J. Snyder, R. V. F. Janssens, M. P. Carpenter, C. J. Chiara, T. L. Khoo, T. Lauritsen, C. J. Lister, D. Seweryniak, S. Zhu, K. Hauschild, A. Lopez-Martens, D. J. Hartley, and S. Frauendorf, Acta Phys. Pol. B **42**, 671 (2011); W. Reviol, D. G. Sarantites, M. Montero, O. Pechenaya, J. Snyder, M. P. Carpenter, C. J. Chiara, R. V. F. Janssens, T. Lauritsen, D. Seweryniak, S. Zhu, D. J. Hartley, K. Hauschild, A. Lopez-Martens, S. Frauendorf, and J. Dudek, Proceedings of Nuclear Structure, 2012 (unpublished).

[20] R. Palit, S. Saha, J. Sethi, T. Trivedi, S. Sharma, B. S. Naidu, S. Jadhav, R. Donthi, P. B. Chavan, H. Tan, and W. Hennig, Nucl. Instrum. Methods Phys. Res., Sect. A **680**, 90 (2012).

[21] D. C. Radford, Nucl. Instrum. Methods Phys. Res., Sect. A **361**, 297 (1995).

[22] A. Kramer-Flecken, T. Morek, R. M. Lieder, W. Gast, G. Hebbinghaus, H. M. Jager, and W. Urban, Nucl. Instrum. Methods Phys. Res., Sect. A **275**, 333 (1989).

[23] L. A. Riley, P. D. Cottle, M. Fauerbach, V. S. Griffin, B. N. Guy, K. W. Kemper, G. S. Rajbaidya, and O. J. Tekyi-Mensah, Phys. Rev. C **62**, 021301(R) (2000).

[24] A. M. Y. El-Lawindy, J. D. Burrows, P. A. Butler, J. R. Cresswell, V. Holliday, G. D. Jones, R. Tanner, R. Wadsworth, D. L. Watson, K. A. Connell, J. Simpson, C. Lauterbach, and J. R. Mines, J. Phys. G **13**, 93 (1987).

[25] E. D. Hackett, J. A. Kuehner, J. C. Waddington, and G. D. Jones, Phys. Rev. C **40**, 1234 (1989).

[26] C. F. Liang, P. Paris, A. Gizon, V. Barci, D. Barneou, R. Beraud, J. Blachot, Ch. Briancon, J. Genevey, and R. K. Sheline, Z. Phys. A **341**, 401 (1992).

[27] W. Nazarewicz, P. Olanders, I. Ragnarsson, J. Dudek, and G. A. Leander, Phys. Rev. Lett. **52**, 1272 (1984).

[28] J. Manns, J. Groger, C. Gunther, U. Muller, T. Weber, and J. de Boer, Eur. Phys. J. **3**, 263 (1998).

[29] N. J. Hammond, G. D. Jones, P. A. Butler, R. D. Humphreys, P. T. Greenlees, P. M. Jones, R. Julin, S. Juutinen, A. Keenan, H. Kettunen, P. Kuusiniemi, M. Leino, M. Muikku, P. Nieminen, P. Rahkila, J. Uusitalo, and S. V. Khlebnikov, Phys. Rev. C **65**, 064315 (2002).

[30] P. Bonche, P. H. Heenen, H. Flocard, and D. Vautherin, Phys. Lett. B **175**, 387 (1986).

[31] A. Bohr and B. R. Mottelson, in *Nuclear Structure* (Benjamin, New York, 1975), Vol. 2.

[32] I. Wiedenhover, R. V. F. Janssens, G. Hackman, I. Ahmad, J. P. Greene, H. Amro, P. K. Bhattacharyya, M. P. Carpenter, P. Chowdhury, J. Cizewski, D. Cline, T. L. Khoo, T. Lauritsen, C. J. Lister, A. O. Macchiavelli, D. T. Nisius, P. Reiter, E. H. Seabury, D. Seweryniak, S. Siem, A. Sonzogni, J. Uusitalo, and C. Y. Wu, Phys. Rev. Lett. **83**, 2143 (1999).